Article:
Spoor, Fred, Leakey, Meave and O'Higgins, Paul (2016) Middle Pliocene hominin diversity: Australopithecus deyiremeda and Kenyanthropus platyops. Philosophical Transactions Of The Royal Society Of London Series B - Biological Sciences. 20150231. ISSN: 1471-2970

https://doi.org/10.1098/rstb.2015.0231

Middle Pliocene hominin diversity: *Australopithecus deyiremeda* and *Kenyanthropus platyops*

Fred Spoor[1,2], Meave G. Leakey[3,4] and Paul O'Higgins[5]

[1] Department of Cell and Developmental Biology, UCL, London WC1E 6BT, UK.

[2] Department of Human Evolution, Max Planck Institute for Evolutionary Anthropology, Leipzig 04103, Germany.

[3] Turkana Basin Institute, PO Box 24926 Nairobi 00502, Kenya.

[4] Department of Anthropology, Stony Brook University, Stony Brook, NY 11794, USA.

[5] Centre for Anatomical and Human Sciences, Department of Archaeology and Hull York Medical School, University of York, York, YO10 5DD

Keywords: hominin evolution; Pliocene; Africa; maxilla; geometric morphometrics; species diversity.

ABSTRACT

Geometric morphometric shape analyses are used to compare the maxillae of the *Kenyanthropus platyops* holotype KNM-WT 40000, the *Australopithecus deyiremeda* holotype BRT-VP-3/1 and other australopiths. The main aim is to explore the relationship between these two specimens and contemporary *Australopithecus afarensis*. Five landmarks placed on lateral views of the maxillae quantify key aspects of the morphology. Generalised Procrustes analyses and principal component analyses of the resulting shape coordinates were performed. The magnitudes of differences in shape and their significances were assessed using Procrustes and Mahalanobis' distances, respectively. Both KNM-WT 40000 and BRT-VP-3/1 show statistically significant differences in maxillary shape from *A. afarensis*, but do so in dissimilar ways. Moreover, the former differs more from *A. afarensis* than the latter. KNM-WT 40000 has a more anteriorly positioned zygomatic process with a transversely flat, and more orthognathic subnasal clivus. BRT-VP-3/1 has a more inferiorly positioned zygomatic process, a slightly retracted dental arcade, but without shortening of the anterior maxilla. These findings are consistent with previous conclusions that the two fossils should be attributed to separate species, rather than to *A. afarensis*, and with the presence of three contemporary hominin species in the middle Pliocene of eastern Africa.

INTRODUCTION

A detailed morphometric study of the maxilla of the 3.5 Myr hominin cranium KNM-WT 40000 from Lomekwi, west of Lake Turkana, showed that this specimen differs significantly from known *Australopithecus* and *Paranthropus* species, and contemporary *A. afarensis* in particular (1). The diagnostic characters include a transversely and sagittally flat and relatively orthognathic subnasal region, anteriorly placed zygomatic processes and small molars. As such this study provides the quantitative and statistical evidence confirming the conclusions of Leakey et al. (2) that KNM-WT 40000 should be attributed to a new species, *Kenyanthropus platyops*, and that hominin taxonomic diversity in eastern Africa extends back well into the middle Pliocene.

Before the announcement of *K. platyops* Brunet et al (3) had proposed that multiple hominin species were present in the middle Pliocene, by attributing a 3.6 Myr mandible fragment and upper premolar from the Koro-Toro area of Chad to a new species, *A. bahrelghazali*, rather than to *A. afarensis* (see [4] for the geological age). A subsequent study of the symphyseal shape of this specimen and a second, undescribed mandible supported this conclusion (5). However, thus far the Chad specimens have not been widely accepted as a separate species because the preserved morphology is limited, and considered to be within the range of variation of *A. afarensis* (e.g. 6, 7).

Strong evidence for middle Pliocene species diversity was provided by the discovery at one of the Burtele localities (Woranso-Mille, Ethiopia) of 3.4 Myr foot bones that are too primitive to belong to *A. afarensis* (8). More recently, Haile-Selassie et al (9) reported 3.5 to 3.3 Myr dentognathic fossils from the Burtele area, and assigned these to a new species, *A. deyiremeda*, but refrained from attributing the partial foot to this taxon as well. Burtele is close to sites of similar age which have produced abundant *A. afarensis* specimens (10), suggesting that two or more species were not only contemporary but may have lived in close proximity as well.

The holotype of *A. deyiremeda* is BRT-VP-3/1, a left maxilla which is reported to differ from *A. afarensis* by an anteriorly positioned zygomatic process and aspects of its dentition, including crown size and shape, as well as the number of premolar roots (9). As such it appears to share several diagnostic features with *K. platyops*, including zygomatic process

position, small first and second molars, and three-rooted upper premolars (9, 11). However, the two species differ in the anterior part of the maxilla, which is flat and non-projecting in *K. platyops* but curved and protruding in *A. deyiremeda*, as in *A. afarensis*.

Based on the broad species descriptions *A. deyiremeda* seems to display a combination of derived features shared with *K. platyops* and more primitive subnasal morphology shared with *A. afarensis* (11). This pattern raises questions about the phylogenetic relationship between the three taxa, the possibility that *K. platyops* and *A. deyiremeda* share a common ancestor in particular, and warrants a more detailed comparison of their type specimens. Hence, in this study we assess the maxillary shapes of KNM-WT 40000 and BRT-VP-3/1, expanding on previous geometric morphometric analyses (1). The two specimens are compared with other australopiths to contextualise their overall morphological affinities, and foremost with *A. afarensis* as the hominin species living closest in time and location. We examine two hypotheses in particular.

1. BRT-VP-3/1 is not significantly different from *A. afarensis* or other australopiths with respect to features of maxillary shape included in the differential diagnosis of *A. deyiremeda* (9), as the null hypothesis to assess the proposal that BRT-VP-3/1 represents a separate species (9).
2. BRT-VP-3/1 does not share aspects of maxillary shape specifically with KNM-WT 40000, as the null hypothesis to assess the proposal that the two specimens share derived morphology (11).

Hypothesis 1 concerns the shape of the maxilla only. Full evaluation of whether *A. deyiremeda* is a valid species requires analyses of all relevant morphological features (9), and this is outside the scope of this study. The status of KNM-WT 40000 as a separate species *K. platyops* was reviewed comprehensively in Spoor et al (1), and is not discussed here specifically.

MATERIALS & METHODS

KNM-WT 40000 and BRT-VP-3/1 are compared with the sample previously used in Spoor et al (1), with the addition of A.L. 822-1. Included are: *A. anamensis* (KNM-KP 29283), *A. afarensis* (A.L. 199-1, A.L. 200-1, A.L. 417-1, A.L. 427-1, A.L. 444-2, A.L. 486-1, A.L. 822-1), *A. africanus* (MLD 9, Sts 52, Sts 71, Stw 498), *A. garhi* (BOU-VP-12/130), *Paranthropus aethiopicus* (KNM-WT 17000), *P. boisei* (OH 5), and *P. robustus* (SK 11, SK 12, SK 13, SK 46, SK 48, SK 83, SKW 11). These are adults, with the exception of A.L. 486-1, Sts 52, OH 5, SK 13 and SKW 11, which are subadults (late juvenile; third molars not in occlusion). BRT-VP-3/1 probably falls in the latter category as well (9). With respect to the morphology quantified here it was found that subadults show the same pattern as adults (1).

The analyses are based on five two-dimensional landmarks, taken from the specimens seen in lateral view: nasospinale (ns), prosthion (pr), the buccal alveolar margin between the canine and third premolar (pc), the buccal alveolar margin between the second and third molar (m23), and the anteroinferior take-off of the zygomatic process (azp), a point most anterior, inferior and medial on the root of the process (figure 1). These landmarks quantify the orientation of the subnasal clivus in the midsagittal plane (ns – pr), the anterior zygomatic process position (azp), and the degree of anterior projection and transverse flatness of the subnasal clivus (pr – pc, or sagittally projected length of the canine and incisor alveolar margin).

The method of landmark acquisition is described in Spoor et al (1), and the distortion-corrected data of KNM-WT 40000 were used here. The landmarks of the newly added *A. afarensis* specimen A.L. 822-1 were taken from a lateral view of the cranial reconstruction (12; courtesy of W. Kimbel and Y. Rak). The landmarks of BRT-VP-3/1 were obtained from parallel projected 3D surface views based on computed tomography of the original fossil (figure 1*b* ; 9, Extended Data Figure 1). Landmark placement was aided by examining a good quality plaster cast of the specimen (courtesy of Y. Haile-Selassie). The midline interalveolar septum of BRT-VP-3/1 is not preserved, and the landmark coordinates of prosthion (pr) can only be estimated using clues from the surrounding morphology. Moreover, the location of the anteroinferior take-off of the zygomatic process (landmark azp) is ambiguous because of the shape of the process. Its surface gently turns from inferiorly facing to somewhat more anteriorly facing at the antero-posterior level of the distal half of P^4. However, it is above the

mesial half of the P^4 that the surface of the process becomes more clearly anteriorly facing, and this level has been described as the anterior margin of the zygomatic root (9). The zygomatic process morphology is best seen in Extended Data Figure 5 of that study, rather than Extended Data Figure 1a reproduced here (figure 1*b*).

To explore how the ambiguous landmark position of pr and azp affects the results two different data sets of BRT-VP-3/1 were analysed (figure 1*b*). Version 'a' uses the best estimate of pr, as well as azp located at the distal P^4 level. In version 'b' pr is placed slightly more posteriorly, at what appears to be the limit of plausible options, and azp is located at the mesial P^4 level. Version 'b' reflects a morphology that is slightly less prognathic than version 'a', and has a more anteriorly positioned zygomatic process, potentially emphasizing similarities to KNM-WT 40000. This version is therefore of particular interest when examining hypothesis 2. The three landmarks other than pr and azp are unambiguous and the same in versions 'a' and 'b'.

Generalised Procrustes analyses (GPA) of the landmark coordinates and principal component analyses (PCA) of the resulting shape coordinates were performed with Morphologika 2.5 (13). The resulting PC plots describe shape differences among BRT-VP-3/1 and KNM-WT 40000 in the setting of the wider sample of australopiths. Differences in shape along the PC axes are visualised using transformation grids which compare a target shape with a reference shape which, in our analyses, usually represents the presumed primitive condition. All described differences relate to relative rather than absolute locations of landmarks with respect to each other (hence shape) since differences in centroid size, translation and rotation have been removed in the analyses.

The magnitudes of differences in shape between the maxillae of BRT-VP-3/1 and KNM-WT 40000 and those of species represented by multiple specimens, *A. afarensis*, *A. africanus* and *P. robustus*, were assessed using Procrustes distances (table 2). The significances of these shape differences were assessed, albeit approximately given small sample sizes, using Mahalanobis' distances calculated from all PCs (in-house software) based on a chi-square distribution and the appropriate degrees of freedom. In Spoor et al (1) the sample size of *A. africanus* was reported to be too small for the software to calculate a probability for differences between this species and KNM-WT 40000. However, we have since found that this was due to an operating system compatibility issue, which is corrected here. Analyses are

restricted to comparisons involving BRT-VP-3/1 or KNM-WT 40000. Others, such as between *A. garhi* and *A. afarensis*, are outside the scope of this study, and relevant species-specific features are not necessarily captured by the data set employed here.

Specific differences and similarities between BRT-VP-3/1, KNM-WT 40000 and *A. afarensis* were explored in two subsequent analyses. First, differences in shape between the maxillae of BRT-VP-3/1 and KNM-WT 40000 and those of the *A. afarensis* sample are examined using PCA. Second, differences in shape between the maxillae of BRT-VP-3/1 and KNM-WT 40000 and that of the *A. afarensis* mean are visualised and compared using PCA and transformation grids.

RESULTS

In the PCA of the full sample (table 1), the first six PCs account for 100% of the variance. PCs 1, 2, 3 and 5 reveal interesting differences among fossils and these are shown in the plots of figures 2-4, with the modes of variation they represent visualised using transformation grids.

The mode of variation represented by PC 1 (70 % of variance) is visualised using a reference grid at the positive limit of PC 1 (0.2) and all other PCs 0, and a target grid at the negative limit (-0.2) of the same PC (figure 2, right and left insets, respectively). The latter shows considerable deformation, including a crease overlying the anterior zygomatic process (azp) and passing diagonally from top to bottom. Moreover, the deformed target grid is taller and the anterior maxilla (pr-pc) relatively shorter and transversely flat, with azp relatively more anterior and the subnasal clivus (ns–pr) decreased in relative length. The crease indicates that there is a large shape difference, particularly in the antero-posterior relationships of azp relative to nasospinale (ns) and the buccal alveolar margin between the canine and third premolar (pc). This together with the changes in the subnasal clivus describes the flattened anterior maxilla and relatively forwardly placed zygomatic root that distinguishes *Paranthropus* from *Australopithecus* species. KNM-WT 40000 is intermediate between the two genera, although close in PC 1 score to the *P. robustus* subadult SKW 11. Both versions of BRT-VP-3/1 fall within the range of *A. afarensis* and version 'b' within that of *A. africanus* as well. Version 'a' of BRT-VP-3/1 falls close to the *A. anamensis* and *A. garhi* specimens.

The mode of variation that PC 2 (14 % of total variance) represents is visualised using a reference grid with PC 2 score -0.15 and a target grid with PC 2 score +0.15 (figure 2). Key features of the deformation include a more anteriorly positioned zygomatic process (azp), and a more inferiorly positioned nasal sill (ns) resulting in relatively reduced maxillary height and moderate shortening of the subnasal clivus (pr – ns). PC 2 separates *A. afarensis*, with a relatively more posteriorly positioned zygomatic, a more superior nasal sill and a longer subnasal clivus, from *A. africanus*, with a more anteriorly postioned zygomatic, a more inferior nasal sill and a shorter clivus. KNM-WT40000 is intermediate. Both versions of BRT-VP-3/1 fall outside the range of *A. afarensis*. They fall within the ranges of *A. africanus* and *Paranthropus*, and version 'a' falls close to the *A. anamensis* and *A. garhi* specimens.

The mode of variation that PC 3 (10% of variance) represents is visualised using a reference grid drawn over the shape with PC3 score -0.13 and a target grid with PC 3 score 0.13 (figure 3). The deformed grid mostly represents marked variation in relative inferosuperior position of the anterior zygomatic process (azp), and as an opposite trend, the inferoposterior position of subnasal segment ns–pr. *A. afarensis, A africanus* and *P. robustus* largely overlap. KNM-WT 40000 falls only just outside the range of *A. afarensis* and within the range of *A. africanus* and *P. robustus*. Both versions of BRT-VP-3/1 fall outside the ranges of *A. africanus* and *A. afarensis*, expressing the relatively inferior position of its anterior zygomatic process. The strongest contrast is with KNM-KP 29283 (*A. anamensis*) and OH 5 *(P. boisei*), which have the most superiorly positioned zygomatic process. Both versions of BRT-VP-3/1 fall within the range of *P. robustus*.

PC 4 (4% of variance; not shown) represents a simple mode of variation of the whole maxilla, whereby taller maxillae have more positive scores and the grid shows a small uniform shear such that the alveolar margin becomes relatively more posteriorly positioned with respect to the other landmarks. There is no clear distinction between *A. afarensis*, *A. africanus* and *P. robustus*. The scores for KNM-WT 40000 and BRT-VP-3/1 fall within range of *A. afarensis*.

PC 5 represents a very small proportion of the total variance (1.6%) but this is not in itself a reason to dismiss it because a single specimen that differs from the rest is expected to contribute to only a small proportion of the total variance and may be differentiated on that axis alone. Here, PC 5 differentiates KNM-WT 40000 from the rest of the sample. This difference is visualised using a reference grid drawn over the sample mean shape with all PC scores 0, and a target grid at PC 5 score -0.7 with 0 for all other PCs, representing KNM-WT 40000 (figure 4). The target grid shows a single localised deformation comprising a relatively inferior deflection of the subnasal clivus orientation (pr–ns) relative to the remaining landmarks. Thus, that KNM-WT 40000 has a lower score on PC 5 than any of the other specimens, indicates that it is subnasally most orthognathic, whereas KNM-WT 17000 (*P. aethiopicus*) and BOU-VP-12/130 (*A. garhi*) are the most prognathic. The other species of *Australopithecus* and *Paranthropus* do not differ notably. Both versions of BRT-VP-3/1 fall within the range of *A. afarensis*, *A. africanus* and *P. robustus*.

PC 6: (1% of variance; not shown) represents variation in the relative anteroposterior position (projection) of prosthion (pr) relative to the remaining landmarks. Both KNM-WT 40000 and BRT-VP-3/1 fall within the largely overlapping ranges of *A. afarensis*, *A. africanus* and *P. robustus*.

To consider the extent to which the foregoing differences between KNM-WT 40000 and BRT-VP-3/1 on the one hand, and *A. afarensis*, *A. africanus* and *P. robustus* on the other are statistically significant Mahalanobis' distances calculated over all PCs were used to estimate significance based on a chi-square distribution and the appropriate degrees of freedom (table 2). KNM-WT 40000 differs significantly from all three species, and as indicated by the Procrustes distances, most from *A. afarensis* and least from *P. robustus*. The 'a' version of BRT-VP 3/1 also differs significantly from all three species, but most from *P. robustus* and the least from *A. africanus*. The 'b' version of BRT-VP 3/1 differs significantly from *A. afarensis* and *P. robustus*, more from the latter than from the former. It is not significantly different from *A. africanus*, even though it lies just outside the range of this species (as seen on PC 3; figure 3).

A specific comparison between the maxillary shape of BRT-VP-3/1 (both versions), KNM-WT 40000 and *A. afarensis* is shown in figure 5. The first two PCs (86% of total variance) clearly differentiate the three, reflecting the highly significant differences suggested by the analysis of Mahalanobis' distances (table 2). PC 1 represents variation in inferosuperior position of the zygomatic process and anteroposterior length of anterior maxilla. PC 2 represents variation in anteroposterior position of the zygomatic process, and the angle of the anterior maxilla (pc – pr - ns) to the postcanine segment (pc - m23). To visualise the differences, *in toto*, a further PCA of shape was carried out in a space with dimensionality reduced by using the mean of *A. afarensis* rather than its individual specimens (figure 6). In the resulting plot of PCs 1 and 2 (98% total variance) a reference grid is drawn over the mean of *A. afarensis* and deformed target grids over KNM-WT 40000 (lower left) and over the mean of both versions of BRT-VP-3/1 (lower right). The PC plot and transformation grids reinforce that KNM-WT 40000 differs from *A. afarensis* in having a more anteriorly positioned zygomatic process (azp) and an anteroposteriorly shortened and inferiorly positioned, more orthgnathic anterior maxilla. In contrast BRT-VP-3/1 differs from *A. afarensis* in having a more anteriorly and inferiorly positioned zygomatic process (azp) without shortening of the anterior maxilla.

DISCUSSION

The geometric morphometric shape analyses of this study compare the maxillae of the *K. platyops* holotype KNM-WT 40000, the *A. deyiremeda* holotype BRT-VP-3/1 and other australopiths. The main aim is to explore whether maxillary shape can provide evidence regarding the relationship between these two type specimens and particularly *A. afarensis*, the well-documented hominin species that is contemporary in eastern Africa. We test the specific hypotheses that (1) BRT-VP-3/1 is not different from *A. afarensis* or other australopiths, and (2) BRT-VP-3/1 and KNM-WT 40000 do not specifically share derived morphology. Before using the evidence obtained here to examine these hypotheses we will briefly summarize the key results of the analyses.

BRT-VP-3/1 stands out in having a zygomatic process that is positioned more inferiorly (PC 3) than in *Australopithecus* and KNM-WT 40000, and more anteriorly (PC 2), compared with *A. afarensis*. PCs 2 and 3 are also associated with the inferosuperior position of the nasal sill (ns), but they show opposite trends which in BRT-VP-3/1 cancel out, reflecting its indistinct sill height. BRT-VP-3/1 differs from *Paranthropus* and KNM-WT 40000 by having a more projecting anterior dental arcade, also seen in *Australopithecus* (PC 1). Moreover, it also differs from KNM-WT 40000 in lacking the orthognathic subnasal clivus of the latter (PC 5). Overall, BRT-VP-3/1 is closest in maxillary shape to *A. africanus*. These conclusions hold for both landmark versions of the specimen.

The results obtained here for BRT-VP-3/1 are consistent with observations reported previously (9), including the position of the anteroinferior take-off of the zygomatic process, the projection of the anterior dental arcade and subnasal prognathism. With respect to the latter, Haile-Selassie et al (9) give a subnasal clivus angle (ns-pr to pc-m23) of 39 degrees, which is the same as that calculated from landmark version ‘a’ used here, and just below the 41 degrees of version ‘b’.

The main PCA in this study yields results similar to that presented previously (1). The addition of BRT-VP-3/1 and *A. afarensis* specimen AL 822-1 results in small differences which mostly concern how certain PCs relate to the position of the zygomatic process (azp). Both the old and new PCAs show that the maxillary shape of KNM-WT 40000 is characterised by an anteriorly positioned zygomatic process with a transversely flat subnasal

clivus when compared with *Australopithecus* (PC 1), and reduced subnasal prognathism when compared with *Australopithecus* and *Paranthropus* (PC 5).

Hypothesis 1 can be assessed most directly using the analyses of Mahalanobis' distances (table 2). These show that BRT-VP-3/1 is significantly different in maxillary shape from *A. afarensis* and *P. robustus*, as well as from *A. africanus* when using version 'a' of BRT-VP-3/1. When using version 'b' the difference from *A. africanus* is statistically not significant. However, it should be noted that this version 'b' concerns a specific ('skewed') interpretation of the morphology of BRT-VP-3/1, which aimed to emphasize similarities to KNM-WT 40000. Comparisons with species other than *A. afarensis*, *P. robustus* and *A. africanus* could not be undertaken using Mahalanobis' distances because each is only represented by a single specimen.

Caution is due in interpreting the species comparisons in the Mahalonobis' distance tests, because of the inevitable small sample sizes which may not fully capture intraspecific variation. Spoor et al (1) made comparisons with much larger samples of modern humans, chimpanzees and gorillas and found that the fossil samples used here do show representative levels of intraspecific morphological variation. Statistical tests take sample size into account and those employed here are conservative in nature. Hence, the fact that statistical significance is obtained for small samples suggests that the observed differences are substantial. Moreover, it is reassuring to note that the pattern of statistically significant differences fits well with the relationships among fossils in the PCA (figures 2-4), and with the Procrustes distances (table 2).

A potential bias in the comparisons of BRT-VP-3/1 could result from its likely status as a subadult (9). When examining the maxillary shape of KNM-WT 40000 the presence of five subadults in the comparative sample was found to have no impact on the results (1). However, BRT-VP-3/1 is characterized by different morphological features, and developmental age needs to be reconsidered with respect to PCs 2 and 3 (anterorposterior and inferosuperior position of the zygomatic process, respectively). In the main PCA the highest PC 2 score of the *A. afarensis* sample is shown by the subadult A.L. 486-1 (table 1). The same holds true for *P. robustus* with respect to the subadults SK 13 and SKW 11, but not for *A. africanus*, where the subadult Sts 52 actually has the lowest score of the species. Hence, there is no consistent pattern indicating that the higher PC 2 score of BRT-VP-3/1 compared

with *A. afarensis* could result from the subadult status of the former. Nevertheless, given the ambiguous evidence in this respect a potential link between zygomatic process position expressed by PC 2 and late juvenile development should be investigated further. It is worth noting that the current results reconfirm that the anteroposterior position of the zygomatic process expressed by PC 1, which distinguishes KNM-WT 40000 from *Australopithecus*, does not differ between subadults and adults. PC 3 scores of BRT-VP-3/1 are notably high, but subadults in the comparative sample do not stand out in this respect.

A second potential source of bias could come from sex differences and an imbalance in male-female representation in the comparative sample. BRT-VP-3/1 is a small maxilla (figure 1), and it could be argued that its particular shape might be that of a small female. If species with which it is compared are mostly represented by larger, more 'robust' males, sex differences could be incorrectly interpreted as taxic diversity. In the analyses of this study the PCs only reflect the shapes of males or females, since size has been removed beforehand. Among the seven specimens of the *A. afarensis* sample are both a large male, A.L. 444-2, and two females, A.L. 417-1 and A.L. 822-1 (10, 12), but their scores on PCs 2 and 3 do not sort according to sex (table 1). The sex of the *A. africanus* specimens used here is uncertain. However, large males are not represented, going by the evidence from the large Stw 505 male (a specimen not included because of its distorted maxilla). The *P. robustus* specimens range from smaller (SKW 11) to large (SK 12), but their PC 2 and 3 scores do not sort according to size (table 1). Lockwood et al (14) classified all as males, noting that only a few females are represented in the fossil record of this species. This could potentially affect comparisons, but not to the extent that it could alter the major difference in maxillary shape between *P. robustus* and BRT-VP-3/1 expressed by PC 1 (figure 2).

Having considered the potential impact of sample size, developmental age and sex, we conclude, on balance, that hypothesis 1 can be rejected with respect to *A. afarensis* and *P. robustus*, as well as, more tentatively, *A. africanus*. Following on from this conclusion we can now turn to the issue of the taxonomic status of BRT-VP-3/1. Attributing the specimen to *A. afarensis* can be seen as the default, given that it was found close to contemporary sites with abundant specimens of that species (9). The statistically significant difference from *A. afarensis* in the position of its zygomatic process is thus particularly relevant, but in itself too limited to be diagnostically conclusive. However, dental dimensions distinguish BRT-VP-3/1 from *A. afarensis* as well, including a mesiodistally shorter P^4, and a buccolingually narrower

M^1 and M^2 (*t*-test, $p < 0.038 – 0.019$; comparing data in Haile-Selassie et al [9] with Kimbel & Delezene [10]). *A. anamensis* specimen KNM-KP 29283 shows a similar relationship to BRT-VP-3/1 with respect to maxillary shape, although with less difference in anteroposterior position of the zygomatic process (PC 2), and more in inferosuperior position (PC 3).

Paranthropus is characterised by uniquely derived facial and dental morphology, and in the current study the *P. aethiopicus* specimen KNM-WT 17000 and the *P. boisei* specimen OH 5 group with *P. robustus*. BRT-VP-3/1 is clearly different from all three species (figure 2; table 2). The *K. platyops* specimen KNM-WT 40000 is closer to *Paranthropus* in maxillary shape than to *Australopithecus* (figure 2; table 2), and clearly differs from BRT-VP-3/1 (figure 4). Their relationship will be specifically considered in the context of hypothesis 2.

Procrustes distances show that BRT-VP-3/1 is closer to *A. africanus* in maxillary shape than to *A. afarensis* or *P. robustus* (table 2). Version 'a' of the specimen also falls close to the *A. garhi* specimen BOU-VP-12/130 for PCs 1 and 2 (figure 2), but less so for PC 3 (figure 3). To appreciate how these similarities should be interpreted it is important to note that geometric morphometric shape analyses are good at demonstrating actual differences between species. Similarities in shape, on the other hand, do not imply conspecificity because the choice of landmarks may not capture the diagnostic characters (15). In this particular case BRT-VP-3/1 shares aspects of maxillary shape with *A. africanus*, but clearly differs from this species in dental size. Its C, P^3 and P^4 are shorter mesiodistally and its M^1 and M^2 are both shorter mesiodistally and narrower buccolingually (*t*-test, $p < 0.036 – 0.0003$; comparing data in Haile-Selassie et al [9] with Kimbel & Delezene [10]). The differences in dental size are even more pronounced between BRT-VP-3/1 and *A. garhi* (9, 16).

In all, the evidence reviewed here is consistent with the attribution of BRT-VP-3/1 to a separate species, *A. deyiremeda*, but the close geographical and temporal proximity to *A. afarensis* will logically raise doubt about the validity of this proposal. A thorough quantitative analysis of all the proposed diagnostic features is therefore needed to provide further support, including a full and detailed survey of the relevant morphological variation in the extensive fossil record of *A. afarensis* (10). For example, the specimens included in the present study were selected based on preservation of all five landmarks (figure 1), which strongly limited the sample size. Now that the shape analysis stresses the importance of

zygomatic process position it will be possible to assess this specific morphology as preserved in more fragmentary fossils and allow comparisons with larger samples.

Hypothesis 2 focuses on the relationship between BRT-VP-3/1 and KNM-WT 40000, and in particular the question of whether or not the maxillary shapes of these two specimens share derived features when compared with *A. afarensis*. Both specimens show statistically significant differences in maxillary shape from that species, KNM-WT 40000 substantially more so than BRT-VP-3/1 (table 2). Importantly, the two are differentiated in different ways, rather than to different degrees. (figures 2-6; table 2). In essence, BRT-VP-3/1 lacks the shorter, more orthognathic anterior maxilla seen in KNM-WT 40000 (figure 4, PCs 1 and 5; figure 6, PCs 1 and 2), and the latter lacks the more inferiorly positioned zygomatic process of BRT-VP-3/1 (figure 3, PC 3; figure 6, PC 1).

What the two specimens appear to share is a more anteriorly positioned zygomatic process, compared with *A. afarensis* (figure 6, PC 2). However, closer scrutiny in a wider comparative setting reveals that this seemingly shared feature actually concerns a different phenomenon in KNM-WT 40000 than in BRT-VP-3/1. Both PC 1 and 2 from the PCA of all fossils (figure 2) are associated with the anteroposterior position of the zygomatic process relative to the postcanine tooth row (azp relative to pc – m23). In fact, PC 1 represents variation of the zygomatic process relative to all other parts of the maxilla, including the full dental arcade, the subnasal area and the nasal sill (azp relative to the other four landmarks). It is along this PC that KNM-WT 40000 and *Paranthropus* differ from all *Australopithecus*, presenting a 'true' anterior position of the process. In contrast, PC 2 is better described as expressing anteroposterior variation of the dental arcade relative to the midface as represented by the zygomatic process and the nasal sill (pr – pc – m23 relative to ns – azp). Hence, here the dental arcade is interpreted as the varying part, rather than the zygomatic process. It is along PC 2 that BRT-VP-3/1 and *A. africanus* differ from *A. afarensis*, presenting a more retracted (posteriorly displaced) dental arcade. The fundamental difference between the relevant morphological variation along PC 1 and PC 2 is perhaps best illustrated by the anteroposterior relationship between the zygomatic process and the nasal sill (azp relative to ns). This relationship varies strongly along PC 1 and remains entirely constant along PC 2 (figure 2).

We conclude that there is no convincing evidence that BRT-VP-3/1 shares specific aspects of maxillary shape with KNM-WT 40000. Thus, hypothesis 2 cannot be rejected, regardless of whether version 'a' or 'b' of BRT-VP-3/1 is considered, even though the latter aimed to emphasize similarities to KNM-WT 40000. These findings do not support the notion that *K. platyops* and *A. deyiremeda* could be directly related phylogenetically (11). That suggestion was based on qualitative character description only, and the current study underlines the importance of using the quantitative and integrated approach of geometric morphometrics to explore if more complex characters are homologous and based on the same underlying morphology.

The current study is limited to the shape of the maxilla, but *A. deyiremeda* is also defined by morphological features of two partial mandibles designated as paratypes (9). Comparing the latter with *K. platyops* would be desirable to further clarify their relationship. No mandibles have been formally attributed to *K. platyops*, but KNM-WT 8556, found at Lomekwi, differs from *A. afarensis* (2, 10), and may well belong to this species. Thus, it will be of interest to compare this specimen, as well as KNM-WT 16006, a second partial mandible from Lomekwi (17), with the mandibles attributed to *A. deyiremeda*. Using newly developed methods to assess conspecificy of mandibles and maxillae (15) it would also be important to investigate the association of KNM-WT 8556 and KNM-WT 16006 with KNM-WT 40000, and of the *A. deyiremeda* paratype mandibles with the holotype maxilla.

In conclusion, the findings of this study quantitatively confirm the previous proposal that BRT-VP-3/1 differs from the contemporary eastern African species *A. afarensis* and *K. platyops* (9), although it is much more similar to the former than to the latter. Since the specimen also cannot be affiliated with other australopiths, these results are consistent with its attribution to a separate species, *A. deyiremeda* (9). If correct, this would imply that three contemporary hominin species were present in eastern Africa during the middle Pliocene, with two of these, *A. afarensis* and *A. deyiremeda*, occurring not only in the same time period, but also in close geographical proximity. This raises the question of how these species could have co-existed over a longer period of time in a stable ecosystem. Niche partitioning, involving diversification of diet, foraging behaviour and habitat preferences are potential factors (11). It is intriguing in this context, that most diagnostic differences between *A. afarensis*, *A. deyiremeda* and *K. platyops* functionally relate to aspects of mastication. Apart from postcanine dental size, the present study particularly highlights morphological

characters used to assess the loading of the masticatory system, including the position of the zygomatic process, variations in the length of the anterior and postcanine dental rows, and the height of maxilla (18-22). Hence, dietary adaptation is a prime candidate as the key to understanding morphological diversity between the three species, although random genetic drift could play as much a role as selection (23).

Data accessibility. The GPA coordinates used in this article are available as the electronic supplementary material.

Author contribution. F.S. and M.G.L. collected data; F.S. and P.O.H. analysed data and wrote the paper; all authors read and edited the paper.

Funding. Financial support was provided by the Max Planck Society.

Acknowledgements. We thank the National Museums of Kenya, the National Museum of Ethiopia, the Transvaal Museum (South Africa), Department of Anatomy, Witwatersrand University (South Africa), the Institute of Human Origins (U.S.A.) for access to specimens in their care. We are grateful to Yohannes Haile Selassie for access to a cast of BRT-VP-3/1 and discussing the morphology of *Australopithecus deyiremeda*, and to Zeray Alemseged, Chris Dean, Jean-Jacques Hublin, William Kimbel, Louise Leakey, Frederick Manthi, Emma Mbua, Heiko Temming, and Lukas Westphal for help with various aspects of this study.

REFERENCES

1. Spoor, F., Leakey, M.G. and Leakey, L.N. 2010. Hominin diversity in the middle Pliocene of eastern Africa: the maxilla of KNM-WT 40000. *Phil. Trans. Roy. Soc. B* 365, 3377-3388.

2. Leakey, M.G., Spoor, F., Brown, F.H., Gathogo, P.N., Kiarie, C., Leakey, L.N., and McDougall, I. 2001. New hominin genus from eastern Africa shows diverse middle Pliocene lineages. *Nature* **410**, 433-440.

3. Brunet, M., Beauvillain, A., Coppens, Y., Heintz, E., Moutaye, A.H.E. and Pilbeam, D. 1996. *Australopithecus bahrelghazali*, une nouvelle espèce d'hominidé ancien de la région de Koro Toro (Tchad). *C. R. Acad. Sci. Paris* **322**, 907-913.

4. Lebatard, A.-E. et al. 2008. Cosmogenic nuclide dating of *Sahelanthropus tchadensis* and *Australopithecus bahrelghazali*: Mio-Pliocene hominids from Chad. PNAS 105, 3226–3231. doi:10.1073/pnas.0708015105

5. Guy, F., Mackaye, H.T., Likius, A., Vignaud, P., Schmittbuhl, M. and Brunet M. 2008 Symphyseal shape variation in extant and fossil hominoids, and the symphysis of *Australopithecus bahrelghazali*. *J Hum Evol* **55**, 37-47.

6. Kimbel, W.K. 2015 The species and diversity of australopiths. In *Handbook of Paleoanthropology Second edition* (eds W. Henke and I. Tattersall), pp. 2071-2105. Heidelberg: Springer.

7. Wood, B and Grabowski, M. 2015. Macroevolution in and around the hominin clade In E. Serrelli and N. Gontier (eds.), Macroevolution, Interdisciplinary Evolution Research 2, Springer. 345-376. DOI 10.1007/978-3-319-15045-1_11

8. Haile-Selassie, Y., Saylor, B.Z., Deino, A., Levin, N.E., Alene, M., & Latimer, B.M. 2012. A new hominin foot from Ethiopia shows multiple Pliocene bipedal adaptations. Nature 483, 565–569.

9. Haile-Selassie, Y., Gibert, L., Melillo, S.M., Ryan, T.M., Alene, M., Deino, A., Levin, N.E., Scott, G. & Saylor, B.Z. 2015. New species from Ethiopia further expands Middle Pliocene hominin diversity Nature 521, 483–488.

10. Kimbel, W.H. and Delezene L.K. 2009 "Lucy" redux: a review of research on *Australopithecus afarensis*. *Yrbk. Phys. Anthropol.* **52**, 2-48.

11. Spoor, F. 2015. The middle Pliocene get crowded. *Nature* **521**, 432-433.

12. Kimbel, W.H. and Rak, Y. 2010. The cranial base of *Australopithecus afarensis*: new insights from the female skull. Phil. Trans. R. Soc. B 365, 3365–3376. doi:10.1098/rstb.2010.0070

13. O'Higgins, P. and Jones, N. 1998 Facial growth in *Cercocebus torquatus*: An application of three dimensional geometric morphometric techniques to the study of morphological variation. *J. Anat*. **193**, 251-272.

14. Lockwood, C. A., Menter, C. G., Moggi-Cecchi, J., & Keyser, A. W. 2007. Extended male growth in a fossil hominin species. *Science* **318**, 1443-1446.

15. Spoor, F., Gunz, P., Neubauer, S., Stelzer, S., Scott, N., Kwekason, A., Dean, M.C. 2015. Reconstructed *Homo habilis* type OH 7 suggests deep-rooted species diversity in early *Homo*. *Nature* **519**, 83-86. doi:10.1038/nature14224

16. Asfaw, B., White, T., Lovejoy, O., Latimer, B., Simpson, S., & Suwa, G. (1999). *Australopithecus garhi*: a new species of early hominid from Ethiopia. *Science* **284**, 629-635.

17. Brown, B., Brown, F. and Walker, A. 2001 A. New hominids from the Lake Turkana Basin, Kenya. *J. Hum. Evol*. **41**, 29-44.

18. Rak, Y., 1983. *The australopithecine face*. Academic Press, London.

19. Demes, B. and Creel, N., 1988. Bite force, diet, and cranial morphology of fossil hominids. *J. Hum. Evol.* **17**, 657-670.

20. Spencer, M.A. and Demes, B., 1993. Biomechanical analysis of masticatory system configuration in Neandertals and Inuits. *Am. J. Phys. Anthrop.* **91**, 1-20.

21. Strait, D. S. *et al*. (2009). The feeding biomechanics and dietary ecology of *Australopithecus africanus*. *Proc. Nat. Acad. Sci.* **106**, 2124-2129.

22. Wroe, S., Ferrara, T.L., McHenry, C.R., Curnoe, D. and Chamoli, U., 2010. The craniomandibular mechanics of being human. *Proc. Roy. Soc. Lond. B: Biological Sciences*, DOI: 10.1098/rspb.2010.0509 .

23. Ackermann, R. R., & Cheverud, J. M. 2004. Detecting genetic drift versus selection in human evolution. *Proc. Nat. Acad. Sci.* **101**, 17946-17951.

Table 1. PCs of the maxillary shape analysis of the full hominin sample. See Material & Methods for species attributions.

	PC 1	PC 2	PC 3	PC 4	PC 5	PC 6
A.L. 199-1	0.127	-0.104	-0.053	-0.004	-0.040	0.018
A.L. 200-1	0.166	-0.048	-0.007	0.005	-0.026	-0.001
A.L. 417-1	0.037	-0.125	0.022	-0.009	0.002	0.019
A.L. 427-1	0.107	-0.070	-0.053	-0.023	-0.002	0.004
A.L. 444-2	0.032	-0.135	-0.010	-0.003	0.019	-0.023
A.L. 486-1	0.181	-0.006	-0.005	-0.011	0.030	0.002
A.L. 822-1	0.123	-0.031	0.007	0.064	0.018	0.004
BOU-VP-12/130	0.161	0.029	0.014	-0.032	0.029	-0.004
BRT-VP-3/1 (a)	0.163	0.027	0.111	0.017	-0.008	-0.009
BRT-VP-3/1 (b)	0.099	0.073	0.078	0.045	-0.007	-0.011
KNM-KP 29283	0.143	0.042	-0.106	-0.040	0.009	0.000
KNM-WT 17000	-0.169	0.066	-0.007	-0.013	0.042	0.018
KNM-WT 40000	-0.084	0.002	0.023	0.037	-0.066	-0.001
MLD 9	0.070	0.044	0.062	-0.008	0.015	0.035
OH 5	-0.218	-0.003	-0.128	0.051	0.000	0.012
SK 11	-0.237	-0.049	0.118	-0.013	0.004	-0.009
SK 12	-0.277	-0.023	0.054	-0.098	-0.014	0.002
SK 13	-0.186	0.073	-0.035	0.013	-0.016	0.000
SK 46	-0.225	-0.065	0.025	0.049	0.023	0.019
SK 83	-0.218	-0.017	-0.056	-0.014	0.008	-0.046
SKW 11	-0.085	0.141	-0.016	0.021	-0.011	0.004
Sts 52	0.111	0.023	0.000	0.032	0.013	-0.035
Sts 71	0.046	0.066	-0.026	0.000	0.006	0.006
Stw 498	0.134	0.088	-0.013	-0.065	-0.027	-0.001

Table 2. Mahalanobis' distance test comparing KNM-WT 40000 and BRT-VP-3/1 with hominin species using all PCs combined. PrD, Procrustes distance; D^2, squared Mahalanobis' distance; SDU, standard deviation units; d.f., degrees of freedom (equal number of non-zero PCs); *p*-value, probability that either of the two fossils belongs to the species. All differences but one (n.s.) are statistically significant at $p < 0.05$.

	PrD	D^2	SDU	d.f.	*p*-value
KNM-WT 40000					
A. afarensis	0.22515	22.078	4.698	6	< 0.0025
A. africanus	0.20090	37.108	6.091	4	< 0.0005
P. robustus	0.14777	13.263	3.641	6	< 0.05
BRT-VP3/1 (a)					
A. afarensis	0.17096	12.569	3.545	6	< 0.05
A. africanus	0.13526	22.284	4.72	4	< 0.0005
P. robustus	0.38327	32.278	5.681	6	< 0.0005
BRT-VP3/1 (b)					
A. afarensis	0.18015	13.895	3.727	6	< 0.05
A. africanus	0.09503	9.184	3.03	4	< 0.1 (n.s.)
P. robustus	0.32341	18.329	4.281	6	< 0.005

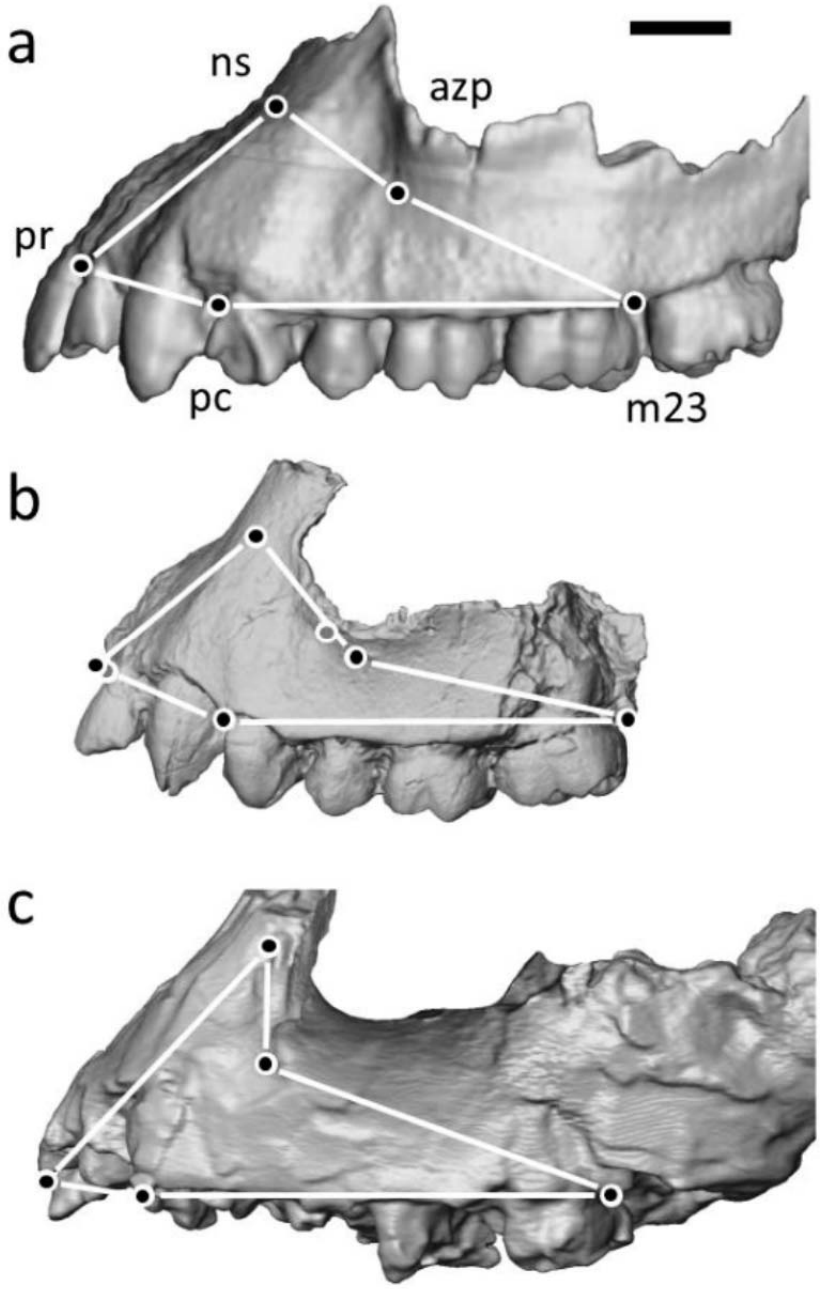

Figure 1. CT-based parallel-projected 3D reconstructions comparing the maxillae in lateral view of a, A.L. 200-1 (reversed right side of cast, *Australopithecus afarensis*), b. BRT-VP-3/1 (left side of original, *A. deyiremeda*; courtesy of Y. Haile-Salassie), and c, KNM-WT 40000 (left side of original, *Kenyanthropus platyops*). The five landmarks are shown, together with the connecting wire frame used in figure 2-4, 6 (see text for the abbreviations of the landmarks). For landmarks pr and azp of BRT-VP-3/1 the black dots represent version 'a' and the grey ones version 'b'. Scale bar 10 mm.

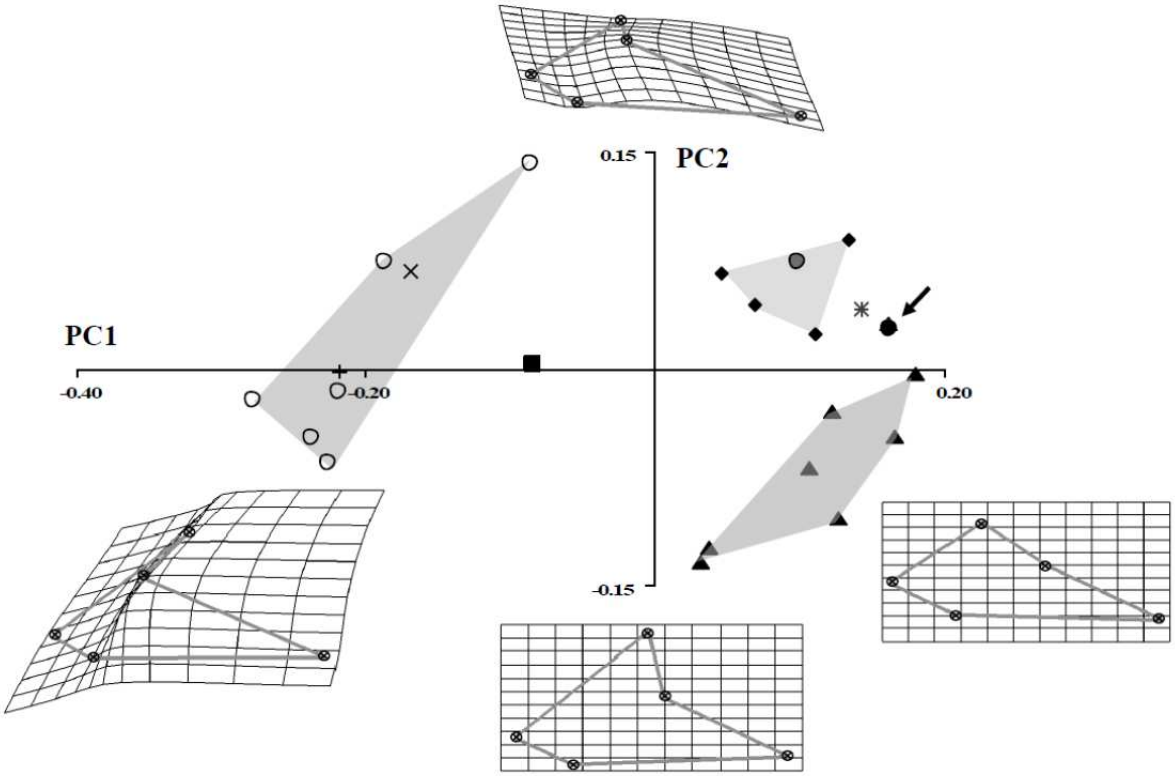

Figure 2. PCA of shape: PC 1 (70% total variance) vs PC 2 (14%). Inset transformation grids, left and right show the warping along PC 1 between a score of 0.2 (reference; regular grid) and -0.2 (target; deformed grid) and along PC 2 between a score of 0.15 (reference; regular grid) and -0.15 (target; deformed grid). BRT-VP-3/1 (black circle, version 'a'; grey circle, version 'b'), KNM-WT 40000 (black square), *A. anamensis* (KNM-KP 29283; asterisk), *A. garhi* (BOU-VP-12/130; open triangle; arrow indicates version 'a' of BRT-VP-3/1 overlying BOU-VP-12/130), *P. boisei* (OH 5; +), *A.aethiopicus* (KNM-WT 17000; X), *A. afarensis* (black triangles), *A. africanus* (black diamond), *P. robustus* (O).

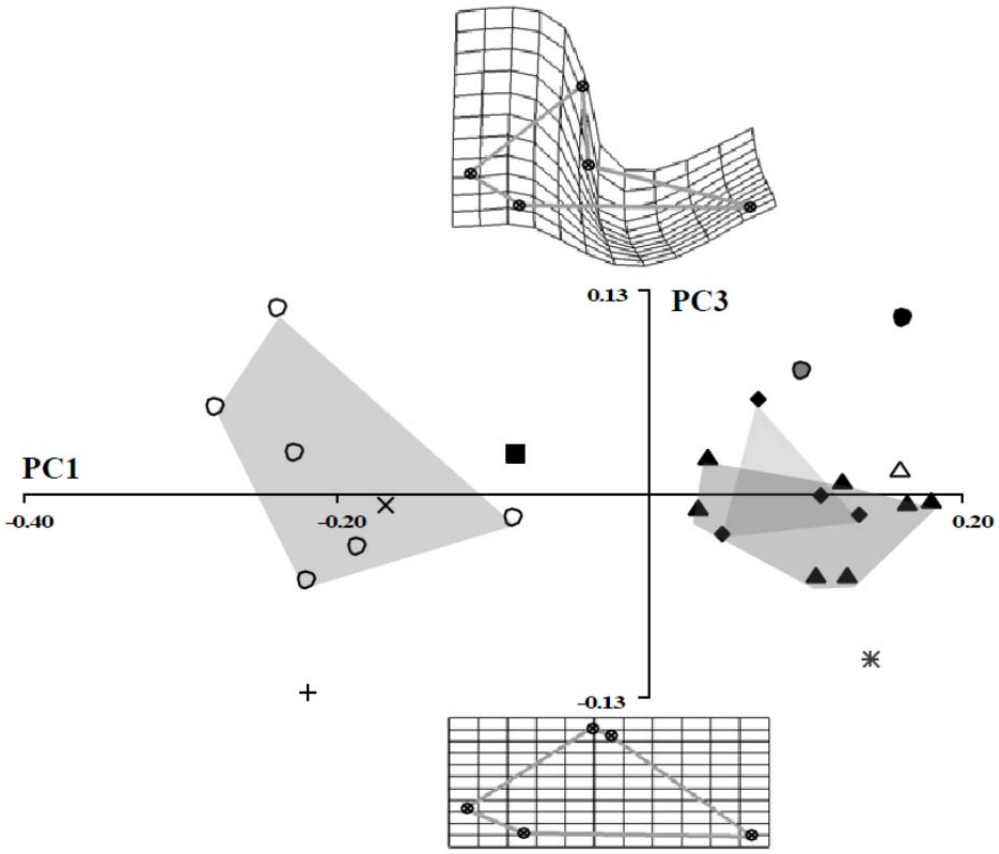

Figure 3. PCA of shape: PC 1 (70% total variance) vs PC 3 (10%). Inset transformation grids show the warping along PC3 between a score of -0.13 (reference; regular grid) and -0.13 (target; deformed grid). Symbols as listed for Figure 2.

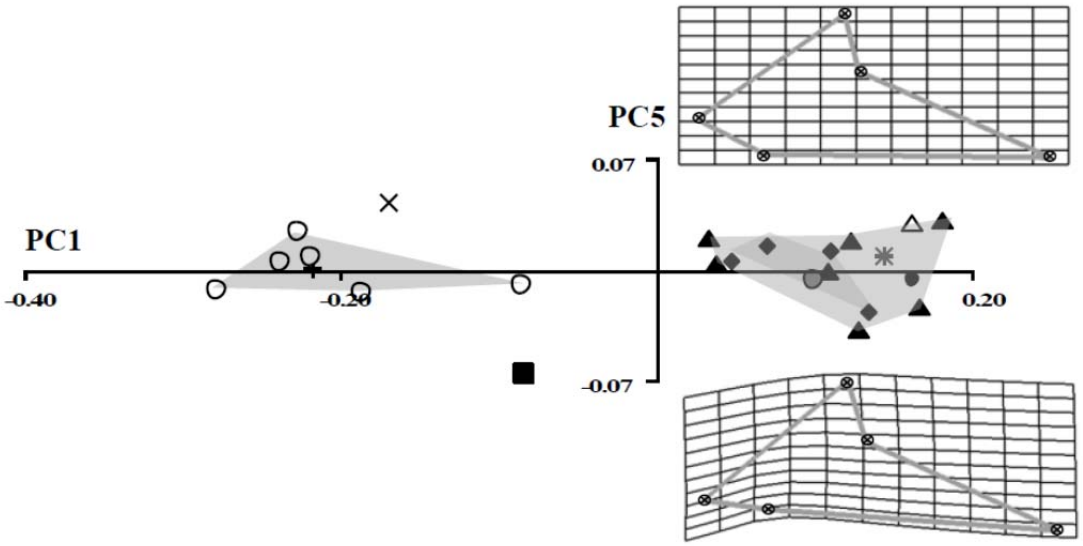

Figure 4. PCA of shape: PC 1 (70% total variance) vs PC 5 (1.6%). Inset transformation grids show the warping along PC5 between a score of 0 (reference; regular grid) and -0.07 (target; deformed grid). Symbols as listed for Figure 2.

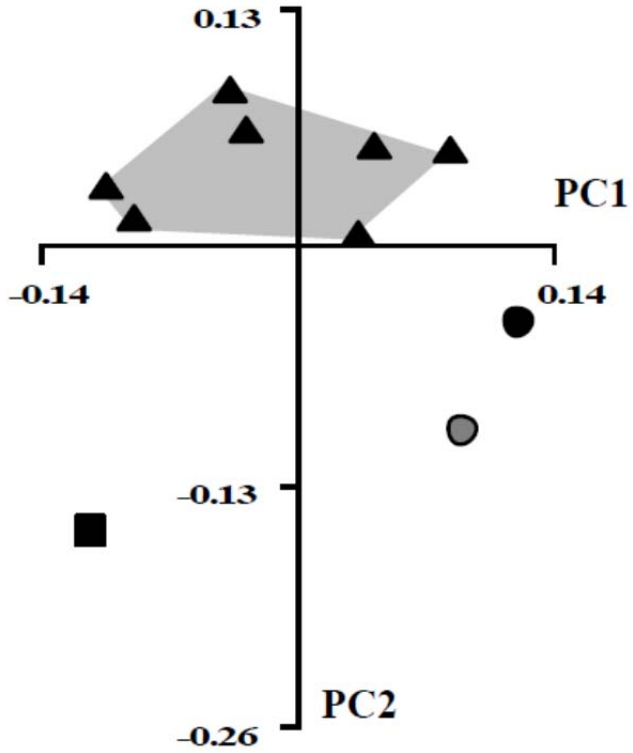

Figure 5. PCA of shape: PC 1 (47% total variance) vs PC 2 (39%).
BRT-VP-3/1 (black circle, version 'a'; grey circle, version 'b'), KNM-WT 40000 (black square), *A. afarensis* (black triangles).

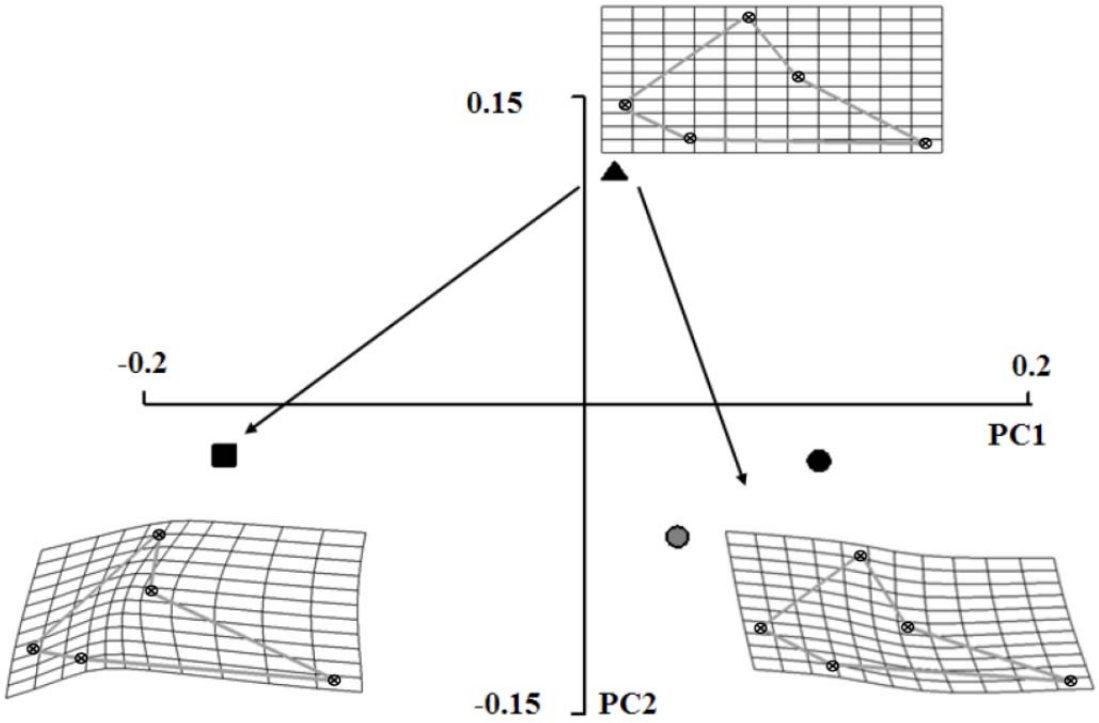

Figure 6. PCA of shape: PC 1 (67% total variance) vs PC 2 (31%). Symbols as indicated for Figure 5. Inset transformation grids show the warping between the *A. afarensis* mean (reference; regular grid), KNM-WT 40000 (target 1; left deformed grid) and the mean position of BRT-VP-3/1 a and b (target 2; right deformed grid).

Supplementary Materials

GPA-coordinates	ns-x	ns-y	pr-x	pr-y	azp-x	azp-y	pc-x	pc-y	m23-x	m23-y
AL199-1	-0.04387	-0.31416	-0.53481	0.08479	0.20625	-0.10589	-0.27568	0.15792	0.6481	0.17733
AL200-1	-0.08514	-0.29603	-0.53669	0.04385	0.18643	-0.07112	-0.24478	0.14583	0.68019	0.17748
AL417-1	0.02121	-0.36134	-0.52021	0.06847	0.13529	-0.05985	-0.28869	0.19426	0.65239	0.15846
AL427-1	-0.02797	-0.28548	-0.54018	0.05758	0.17531	-0.11261	-0.27476	0.17339	0.66761	0.16713
AL444-2	0.03892	-0.34924	-0.55182	0.07013	0.13525	-0.08476	-0.26009	0.20511	0.63773	0.15876
AL486-1	-0.0963	-0.25693	-0.53369	-0.00571	0.17492	-0.07334	-0.24356	0.17183	0.69863	0.16415
AL822-1	-0.08416	-0.32669	-0.51627	0.0224	0.13745	-0.08652	-0.22085	0.19361	0.68383	0.1972
BOUVP12/130	-0.08747	-0.24007	-0.52676	-0.0134	0.14258	-0.06211	-0.2499	0.15727	0.72155	0.15831
BRTVP31a	-0.11529	-0.30303	-0.50693	-0.01068	0.11194	0.00924	-0.21802	0.13147	0.72831	0.17299
BRTVP31b	-0.09986	-0.29679	-0.48797	0.00171	0.05406	-0.04461	-0.21117	0.14076	0.74494	0.19893
KNM-KP29283	-0.07467	-0.19207	-0.52898	0.02625	0.16105	-0.16323	-0.26454	0.15284	0.70714	0.17621
KNM-WT17000	0.09306	-0.28323	-0.43565	0.05072	-0.0837	-0.15562	-0.29729	0.2057	0.72357	0.18244
KNM-WT40000	0.03195	-0.35133	-0.46622	0.1099	-0.00944	-0.10959	-0.26357	0.13882	0.70728	0.21219
MLD9	-0.05955	-0.28929	-0.47409	0.00214	0.06811	-0.05173	-0.27462	0.16496	0.74014	0.17392
OH5	0.12378	-0.31421	-0.43846	0.13404	-0.05757	-0.26201	-0.28117	0.2192	0.65341	0.22298
SK11	0.16712	-0.39263	-0.43943	0.09043	-0.11209	-0.0419	-0.29194	0.18718	0.67633	0.15691
SK12	0.21435	-0.32238	-0.43125	0.11424	-0.11854	-0.08674	-0.34682	0.15924	0.68226	0.13565
SK13	0.08978	-0.29017	-0.43423	0.09657	-0.09375	-0.18498	-0.2801	0.16946	0.7183	0.20913
SK46	0.14256	-0.39997	-0.43468	0.10268	-0.0751	-0.12963	-0.2845	0.23562	0.65171	0.19129
SK83	0.16443	-0.30637	-0.48427	0.11645	-0.07349	-0.18471	-0.27446	0.19298	0.66779	0.18165
SKW11	0.00092	-0.25209	-0.43673	0.04962	-0.06533	-0.16409	-0.25791	0.15023	0.75906	0.21633
Sts52	-0.07247	-0.27794	-0.53238	0.01715	0.10282	-0.09541	-0.20956	0.16442	0.7116	0.19178
Sts71	-0.04439	-0.25195	-0.49177	0.02871	0.06112	-0.131	-0.25994	0.16161	0.73498	0.19262
Stw498	-0.08385	-0.1968	-0.50788	0.01717	0.11328	-0.09035	-0.27167	0.10255	0.75011	0.16742